

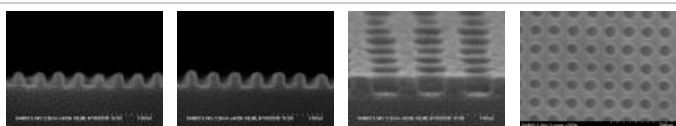
Research

 [Printer-friendly version](#)  [PDF version](#)

CXRO engages in a variety of research areas with the aim of furthering knowledge and applications of x-ray optics. In addition to the topics listed here, further information can be found in the pages describing our [laboratories](#) and [beamlines and endstations](#).

EUV Lithography at the SEMATECH-Berkeley Microfield Exposure Tool Facility (BMET)

 [Printer-friendly version](#)  [PDF version](#)



20nm

22nm

30nm

30nm

Addressing Critical Areas in EUV Lithography Research

The top three critical roadblocks on the path to realizing large-scale manufacturing use of EUV lithography, as identified by the 2008 International EUVL Steering Committee, are:

1. A reliable high-power source and collector module.
2. **The availability of defect-free masks.**
3. **Criteria for resist resolution, sensitivity, and Line Edge Roughness (LER) must be met simultaneously.**

The BMET focuses on the second and third of these issues. Resolution and sensitivity are largely solved issues, though LER still remains a challenge (see [The World's Highest Resolution Projection EUV Lithography Tool](#), and [Resist Development](#)). Progress has been made in making defect-free masks (see [Mask Development](#); CXRO also contributes to this field using the [the Actinic Inspection Tool](#)).

Lithography is the process by which a circuit pattern is transferred into silicon to produce computer chips. Lithography tools can be thought of as Xerox machines for computer chips. Extreme ultraviolet (EUV) lithography [1] uses light of 13.5 nm and is the leading candidate for high volume manufacturing of nano-electronics at feature sizes of 22 nm and below. To make this a reality, advanced research tools operating with numerical apertures (NA) of 0.25 or greater are required today. To address this issue, CXRO has developed a 0.3-NA EUV microexposure tool. This tool uses the Advanced Light Source (ALS) as its source of EUV radiation. The CXRO exposure station is designed to be capable of 12-nm equal-line-space printing.

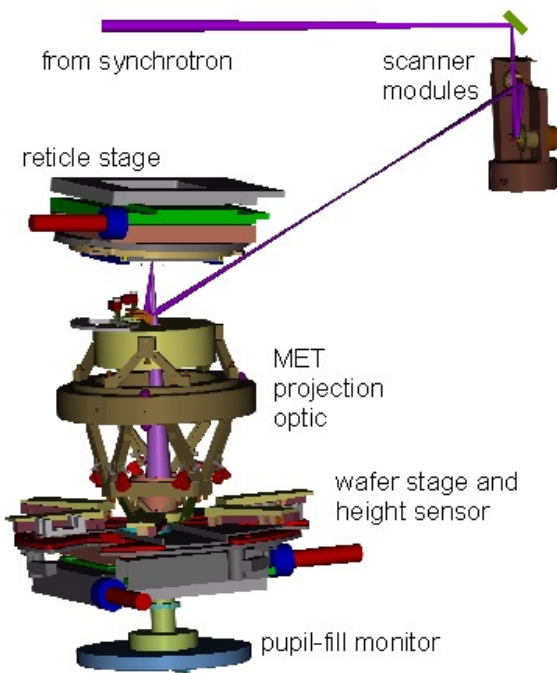


Figure 1: The MET system.

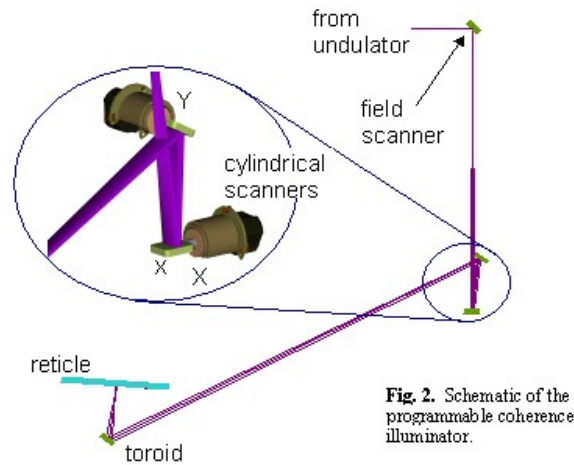


Fig. 2. Schematic of the programmable coherence illuminator.

Figure 1 shows a CAD model of the exposure system depicting the major components as well as the EUV beam path [2]. Effectively coherent radiation from ALS undulator beamline 12 [3,4] impinges on the scanning illuminator. The light is directed to a reflective reticle. From there the light is re-imaged by the all-reflective 0.3-NA optic with 5 \times demagnification to the wafer plane. A grazing incidence laser system is used to monitor the height of the wafer at the print site ensuring that it remains in focus. With the wafer removed, the light propagates to a scintillator plate sitting effectively in the far field. Pupil-fill monitoring is achieved by re-imaging the scintillator plate through a vacuum window to a visible-light CCD camera. A significant difficulty with using a synchrotron source for lithography, however, is the poor match between the intrinsically high coherence of the source as compared to the partial coherence requirements of a lithographic tool. Directly using synchrotron sources would typically limit one to coherence factors below 0.1. To overcome this issue, an active scanning illuminator has been developed (Fig. 2). The use of this scanning illuminator allows lossless variable illumination in patterns such as Fig. 3, as well as those presented on the next page ("The World's Highest Resolution Projection EUV Lithography Tool").

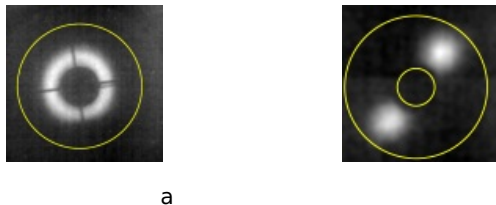


Fig. 3: Illustrations of lossless variable illumination using the scanning illuminator.

Select an image to view it full-size.

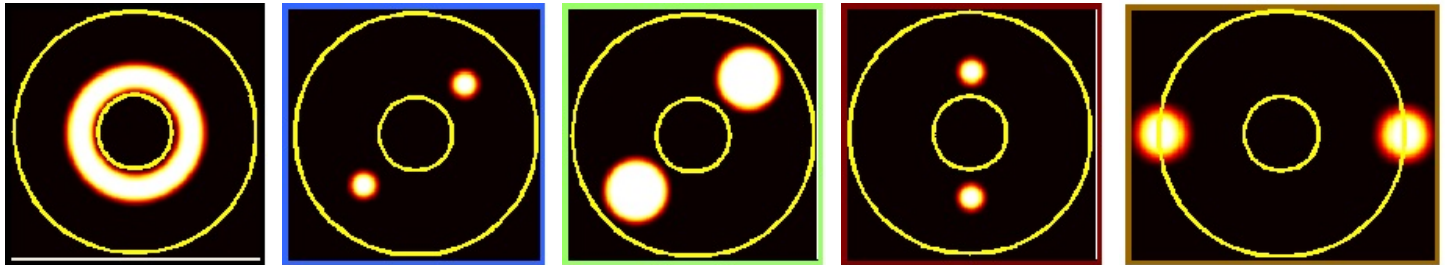
References This research was supported by International Sematech.

1. R. Stulen and D. Sweeney, "Extreme ultraviolet lithography," IEEE J. Quantum Electron. 35, 694-699 (1999).
2. P. Naulleau, K. Goldberg, E. Anderson, et al., Proc. SPIE Vol. 5374, 881-891 (2004).
3. D. Attwood, G. Sommargren, R. Beguiristain, K. Nguyen, J. Bokor, N. Ceglio, K. Jackson, M. Koike, and J. Underwood, "Undulator radiation for at-wavelength interferometry of optics for extreme-ultraviolet lithography," Appl. Opt. 32, 7022-7031 (1993).
4. C. Chang, P. Naulleau, E. Anderson, and D. Attwood, "Spatial coherence characterization of undulator radiation," Opt. Comm. 182, 24-34 (2000).
5. P. Naulleau, K. Goldberg, E. Anderson, J. Cain, P. Denham, K. Jackson, A. Morlens, S. Rekawa, F. Salmassi, "EUV microexposures at the ALS using the 0.3-NA MET optic," J. Vac. Sci. & Technol. B, in review (2004).
6. J. Cain, P. Naulleau, C. Spanos, "Advanced metrology for characterization of extreme ultraviolet lithography process effects," J. Vac. Sci. & Technol. B, in review (2004).
7. R. Soufli et al., Appl. Opt. 46, 3736 (2007)

The World's Highest Resolution Projection EUV Lithography Tool

The SEMATECH-Berkeley MET achieves its world leading performance through the precise manipulation of illumination coherence. Through the use of the unique scanner module and undulator radiation from the [ALS](#), lossless variable illumination can be achieved in patterns such as those pictured here.

Synthesized Pupil Fill Functions

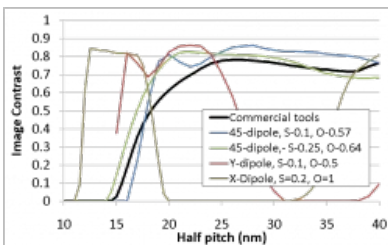


45-dipole, $S=0.1$,
 $O=0.57$

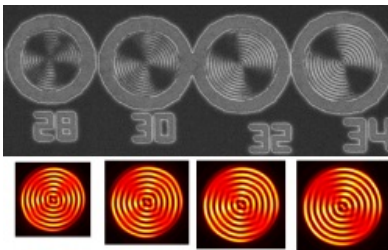
45-dipole, $S=0.25$,
 $O=0.64$

Y-dipole, $S=0.1$, $O=0.5$

X-dipole, $S=0.2$, $O=1$



This coherence control has been demonstrated experimentally at the BMET, as can be seen by comparing the predicted aerial images with actual printing results:



Resist Development

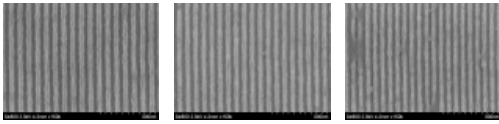
Future generations of computer chips will be manufactured with stringent requirements on three parameters: **Resolution**, **Sensitivity**, and **Line Edge Roughness (LER)**. All three must be met and balanced, or the chips cannot be made. The following table summarizes the goals for each as laid out in the 2007 ITRS Roadmap:

Year	Resolution	LER	Sensitivity
2013	32-nm half pitch (21-nm iso)	1.2 nm	10 mJ/cm ²
2016	22-nm half pitch (15-nm iso)	0.8 nm	10 mJ/cm ²
2019	16-nm half pitch (11-nm iso)	0.6 nm	10 mJ/cm ²

The Berkeley MET tool has been instrumental in improving resists so that resolution is now approaching 20 nm HP using 50 nm thick resists

	24 nm HP	22 nm HP	20 nm HP
Resist C 12.7 mJ/cm ²			

Resist D
15.2 mJ/cm²



Contacts have also been printed 30 nm across at a variety of half-pitches

	45 nm HP	40 nm HP	35 nm HP	30 nm HP
1:1				Resist E 80-nm film thickness
1:1.5				

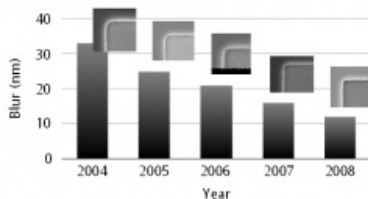
Further demonstrations of high pattern fidelity at small feature sizes

24 nm HP	22 nm HP	20 nm HP
30 nm 1:1 contacts		

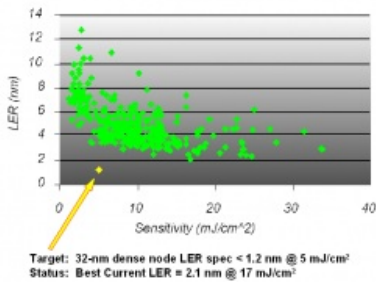
Line-space resolution: Progress over Time ([Click to see full-size images](#))

Year	40 nm Half-pitch	36 nm Half-pitch	32 nm Half-pitch	Annular Illumination
2006				16% 200nm DOF
2007				15% EL 200 nm DOF
2008				8% EL 150 nm DOF

To characterize the performance of resists, systematic contact and corner resist blur metrics have been developed. Steady improvements in resist performance can be seen by comparing these metrics over time:



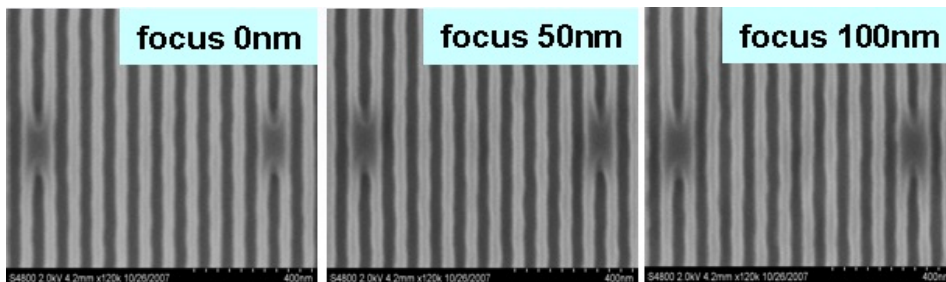
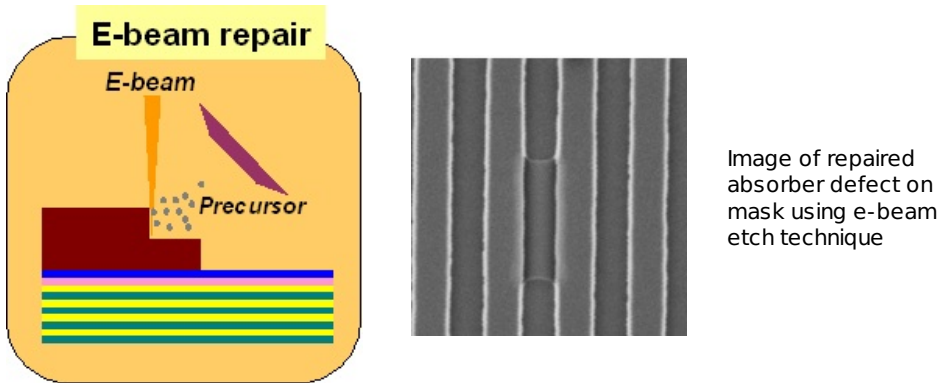
In contrast to the impressive improvements in resolution, line edge roughness (LER) remains the most difficult challenge facing EUV resists. This can be visualized by comparing LER to sensitivity for various resists to the target of LER < 1.2 nm at 5 mJ/cm² on 32 nm dense nodes:



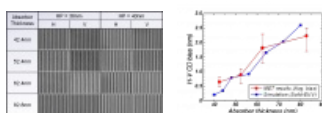
Mask Development

[Printer-friendly version](#) [PDF version](#)

The SEMATECH Berkeley MET is used for the testing of mask repair methods. Masks have been repaired using E-beam etching, then used to print through-focus images in resists, demonstrating the effectiveness of the repair.



The SEMATECH Berkeley MET has also been used to verify mask shadowing models: **(Select an image to view full size)**



References

1. Gi-Sung Yoon et al., 2007 International EUVL Symposium, 28-31 October 2007, Sapporo, Japan
2. Hwan-Seok Seo et al. EIPBN 2008

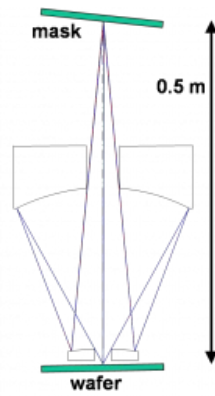
0.5 NA Tool: Pushing EUV Research to the Next Level

[Printer-friendly version](#) [PDF version](#)

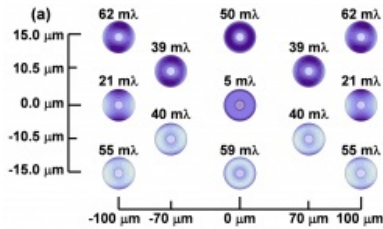
The next level of EUV Lithography research will require even greater resolution and control of optical aberration than is currently achieved. This will require building the successor to the Sematech-Berkeley MET facility, for which the optic design has been completed and optics manufacturers have been engaged. The new design will have:

Optical model courtesy of Russ Hudyma, Hyperion

- **NA = 0.5**
- **Resolution = 8 nm**
- **Magnification = 5x**
- **Field of View = 200x30 m**
- **Mask angle of incidence = 6**

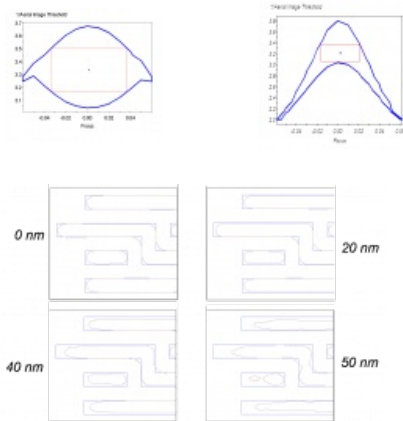


The design aberration across the field of view has been calculated courtesy of Michael Goldstein, SEMATECH:



Sizable process windows, for 12-nm features using conventional illumination

70 nm DOF on 12 nm dense lines **40 nm DOF on 12 nm iso lines**



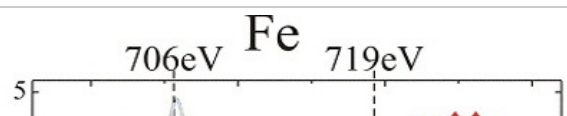
Magnetic Soft X-Ray Microscopy

[Printer-friendly version](#) [PDF version](#)

Modern magnetic materials with applications to magnetic storage and sensor technologies are currently focusing on thin films and multilayered systems often accompanied with a lateral micropatterning. Imaging magnetic microscopic processes on a sub-micrometer length and sub-ns time scale provides key information that will contribute significantly to a thorough understanding of the underlying physics and will support current technological developments.

Magnetic transmission soft X-ray microscopy offers a superior combination of the following features which match ideally the needs both for fundamental studies in magnetism and to characterize technologically relevant magnetic systems

- high lateral resolution (Fresnel zone plate optical elements)
- sub-ns time resolution (pulsed time structure of Synchrotron radiation)
- elemental specificity (XMCD contrast)
- high sensitivity to thin layers (large magnetic absorption cross section)
- magnetisation reversal studies (recording images in applied magnetic fields)
- large field of view (typical tens of microns)
- short exposure times (typical secs per image)

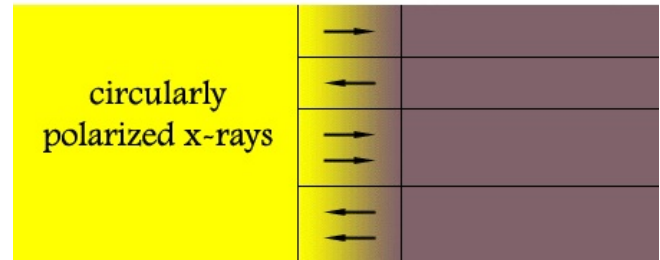
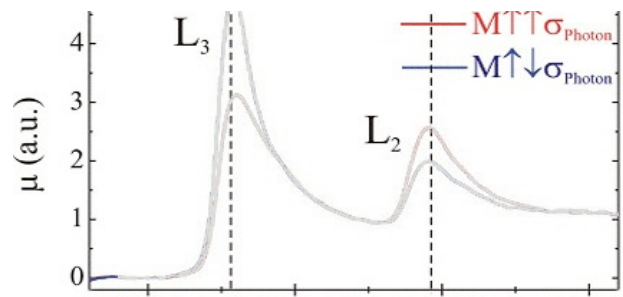


Magnetic transmission X-ray microscopy (MTXM) uses X-ray magnetic circular dichroism as magnetic contrast mechanism. In the vicinity of element-specific binding energies of inner core levels, such as $2p_{3/2}$ and $2p_{1/2}$ levels which correspond to L_3 and L_2 absorption edges, the X-ray absorption coefficient depends strongly on the relative orientation between the helicity of the photons and the projection of the local magnetization onto the photon propagation direction.

With phase sensitive X-ray optics, also magnetic phase contrast imaging has been demonstrated recently.

Principle of MTXM

Illuminate a ferromagnetic specimen with circularly polarized X-rays at a specific wavelength and record the transmitted photons with a high resolution soft X-ray microscope.

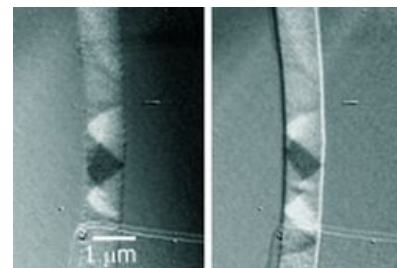




Examples of Recent Results

Direct Imaging of Stochastic Current Induced Domain-Wall Motion

Pulses of nanosecond duration and of high current density up to 1.0×10^{12} A/m² are used to move and to deform the domain wall. The current pulse drives the wall either undisturbed, i.e., as composite particle through the wire, or causes structural changes of the magnetization. Repetitive pulse measurements reveal the stochastic nature of current-induced domain-wall motion.

G. Meier, et al., *Phys. Rev. Lett.* **98**, 187202 (2007), also selected for *Physical Review Focus*




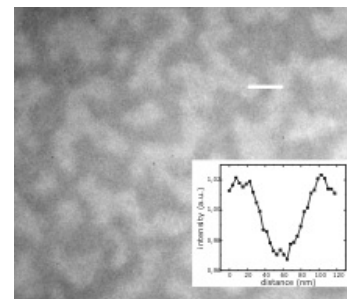
In collaboration with  and 

Imaging at fundamental magnetic length scales

With a spatial resolution of 15nm magnetic soft X-ray microscopy can probe local hysteresis behaviour on a granular length scale in a 50 nm thick (Co₈₃Cr₁₇)₈₇Pt₁₃ nanogranular alloy film recorded at the Co L_3 absorption edge (777eV). Inset: Intensity profile across a magnetic domain (white line) proofing 15nm spatial resolution.

D.-H. Kim, et al. *J. Appl. Phys.* **99**, 08H303 (2006) also selected in *Virtual Journal of Nanoscale Science & Technology*, **13**(17) May 1, 2006

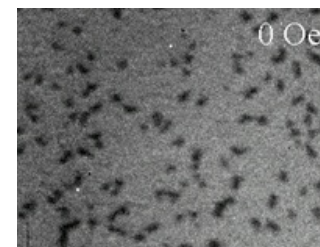
In collaboration with 

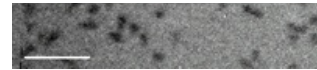


Domain nucleation in nanogranular CoCrPt alloys

The image shows the magnetic domain pattern in a 50 nm thick (Co₈₃Cr₁₇)₈₇Pt₁₃ nanogranular alloy film recorded at the Co L_3 absorption edge (777eV) in an external magnetic field of 0 Oe.

M.-Y. Im, et al. *Appl. Phys. Lett.* **83**(22) (2003) 4589-4591 also selected in *Virtual Journal of Nanoscale Science & Technology*, **8**(23)





Cobalt antidot arrays

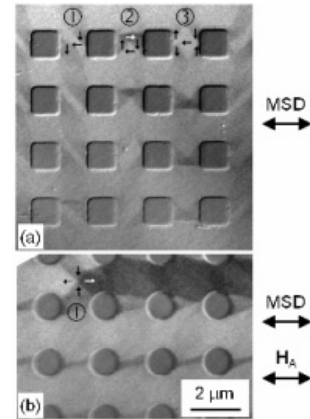
Co antidot arrays with 2 mm period were fabricated on X-ray transparent membranes and imaged with MTXM:

(a) as-grown flux closure states in array with square holes: S-state at position 1, Landau state at position 2, flower state at position 3

(b) a domain chain forms on application of a magnetic field with the end of the chain comprising four 90° walls.

L. Heyderman et al., *J. Magn. Magn. Mat* 316 99 (2007)

In collaboration with  at 



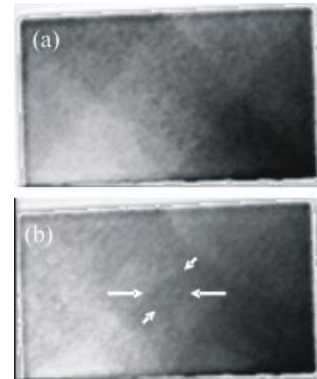
Fast Magnetization Dynamics in Patterned Elements

(a) Seven domain Landau configuration in a 50nm thin 2x4 mm² rectangular PY element before a magnetic excitation.

(b) Domain configuration 2ns after the excitation pulse.

P. Fischer, et al *J. Magnetism and Magnetic Materials* (2007) **310(2)** pt 3 (2007) 2689-2692

In collaboration with 



Multilayer Optics

 [Printer-friendly version](#)  [PDF version](#)

Research on multilayer coatings for x-ray mirrors is one of the principal activities of the Center for X-ray Optics. If you are not familiar with the principles of these optics, or would like to refresh your memory, you may want to have a look at this [mini-tutorial](#).

CXRO has been making, testing and utilizing multilayer x-ray mirrors since 1984, and has made major contributions to understanding the physics and chemistry of these devices, and to their utilization in optical systems for a variety of research fields, including x-ray astronomy, plasma spectroscopy, x-ray lasers and synchrotron radiation research. CXRO has constructed several beamlines at the Advanced Light Source which either utilize these optics or are designed to test them and evaluate their performance. The *X-ray Microprobe Beamline* is in the first category, while the *Calibration and Standards Beamline* and the *EUV Interferometry Beamline* are in the second. CXRO also maintains other instrumentation for the test and evaluation of multilayer mirrors, including a 2-circle x-ray diffractometer operating at 8.0 keV (Cu K α -rays), a soft x-ray reflectometer using a laser-produced plasma as a source, and instruments for the measurement of mechanical properties such as film stress.

Some of the advances made by CXRO in the past few years include:

- Completion of the *Calibration and Standards Beamline* at the Advanced Light Source for the measurement of the properties of multilayers and other x-ray optical components.
- Development of multilayer mirrors to focus x-rays to a 1 micron spot size in an x-ray microprobe.
- Mo/Be multilayers with high reflectance at 110 eV, in a joint development (with Lawrence Livermore National Lab.).
- Development of a dispersion element for the analysis of light elements in an x-ray electron microprobe.
- Coating of Schwarzschild optics for Super-Maximum photo-electron microscope at the Elettra synchrotron radiation facility in Trieste, Italy.
- Research on new combinations of materials to achieve multilayers with special properties or for particular spectral regions.

The primary contact for this project is emgullikson [at] lbl [dot] gov (Eric Gullikson).

Specialized Diffractive Optics



Specialized diffractive optical elements are being developed to improve contrast and resolution for imaging studies in the soft x-ray region. The techniques are developed at the [spatially coherent soft x-ray test station](#), the [full-field soft x-ray microscope XM-1](#), and the [CXRO nanofabrication facility](#) and can be extended for use with compact sources. Both lens based imaging methods utilizing unconventional zone plates and lens-less imaging methods employing improved reference objects are being pursued.

For high resolution lens based imaging, three classes of zone plates are being studied:

- [spiral zone plates](#),
- [Zernike zone plates](#), and
- [wavefront coded zone plates](#).

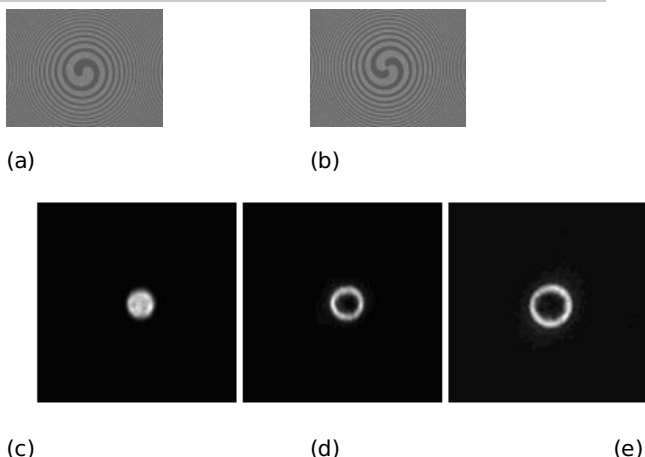
Each of the optics, serving as the single objective lens in the imaging system, performs both the imaging and an additional image processing capability. For example, the spiral zone plates provide a method to image the object's local gradient of refractive index, being sensitive to changes in both phase and amplitude in a specimen. The Zernike zone plates allow soft x-ray Zernike phase contrast imaging without the use of an additional phase ring, and the wavefront coded zone plates allow depth of field extensions for high resolution three dimensional imaging. In addition, resolution and signal to noise improvements for lens-less imaging methods, such as holography, are being made through the use of the [uniformly redundant array](#).

For more information, please see the [publications](#).

Spiral Zone Plate Microscopy

Spiral zone plate (SZP) microscopy has been demonstrated at the [coherent soft x-ray test station](#). Images of a gold pinhole were taken using a regular zone plate, charge 1 SZP, and charge 2 SZP. Edge enhancement as expected is seen in the cases of the SZP images.

Fig. 1: (a) SEM image of a charge 1 SZP, (b) SEM image of a charge 2 SZP, and resulting images of a gold pinhole taken using a (c) Regular zone plate, (d) Charge 1 SZP, (e) Charge 2 SZP.
(Click on an image to view the full-size version)

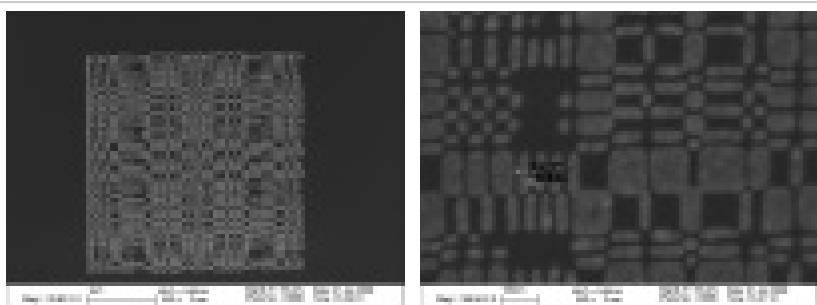


Uniformly Redundant Arrays

Holography performed with uniformly redundant arrays (URA) increase the signal to noise ratio of the holographic signal, which is especially important for high resolution holograms. It can be thought of as a type of multi-reference feature (as seen in figure 4) with the highest possible resolution proportional to the smallest feature sizes on the URA. High resolution URAs have been fabricated and are shown below. Experiments to perform high resolution holography using these URAs are underway.

Fig 4: (left) SEM image of a high resolution uniformly redundant array (URA) to be used as the reference structure for high resolution

soft x-ray holography, (right) a zoomed-in version of the URA structure detailing the small gap sizes allowing for high resolution. (Click on an image to view the full-size version)

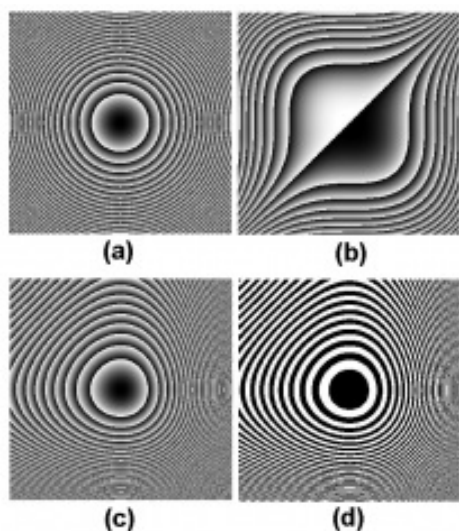


Wavefront Coded Zone Plates

[Printer-friendly version](#) [PDF version](#)

Wavefront coded zone plates (WCZP) are being used to extend depth of field in the [full-field soft x-ray microscope](#). Currently, WCZPs with a cubic phase (as shown in figure 3) have been made and experiments at the full-field soft x-ray microscope are being performed.

Fig. 3: Simulations used in the design of the wavefront coded zone plates (WCZP) (a) a regular zone plate, (b) cubic phase, (c) combination of the regular zone plate and the cubic phase to make the WCZP, (d) a binarized version of the WCZP. (Click on the image to view the full-size version)



Zernike Zone Plates

[Printer-friendly version](#) [PDF version](#)

Zernike phase contrast has been demonstrated using both a positive zernike zone plate (PZZP) and a negative zernike zone plate (NZZP) at the [coherent soft x-ray test station](#). Images of a Cr test sample are shown in Fig. 2 with the corresponding zone plate used. Both contrast enhancement in the case of the PZZP and contrast reversal in the case of the NZZP were demonstrated.

Fig 2. (a) SEM images of a regular zone plate (RZP), positive zernike zone plate (PZZP), and negative zernike zone plate (NZZP) along with corresponding images of a chromium grating test sample (b). Lineouts are shown on the graph to the right. (Click on an image to view the full-size version)

